

and is therefore independent of  $\lambda$  with the enhanced value  $2.97 (K_{e0})^2$ , then agreement with the experimentally observed value of  $K_e^2 T_{1z} T/A$  (Table III) is obtained when  $\lambda = (1.0)2k_F$  and  $\epsilon = 0.05$ . Best agreement between theory and experiment for  $\delta$  is obtained at  $\lambda = (0.42)2k_F$ , with  $\delta = 2.07$ , almost within range of the error in the experimental value. Unfortunately, agreement is then lost between theoretical prediction and experiment for the Korringa product, with  $(K_e^2 T_{1z} T)/A = 2.23$ . The same difficulty is encountered with the Gaussian interaction.

## VII. CONCLUSION

In sodium, the electron-gas theory of electron-spin correlations, including electron-electron interactions of  $\delta$ -function type, fails to explain the experimentally observed enhancements of the Korringa product and the ratio of Zeeman to dipolar spin-lattice relaxation times. Closer agreement between experiment and theory is obtained by imposing a finite range for the electron-electron interactions on to the theory.

In aluminum, we have discussed in some detail the

different contributions to the relaxation time and the Knight shift and have measured  $\delta$  at  $2.15 \pm 0.07$ . A  $\delta$ -function electron-electron interaction produces quite reasonable agreement between theory and experiment in this case, where the Korringa enhancement is abnormally low. Taken with the susceptibility analysis, this leads us to conclude tentatively that the conduction electrons in aluminum interact over a shorter range than in sodium, but that the enhancement of the Knight shift and spin susceptibility is very similar in the two metals.

There has been one other recent determination<sup>27</sup> of  $\delta$  in Al, finding a value of  $2.07 \pm 0.02$  at  $273^\circ\text{K}$ . This value and ours overlap, though we think this fortuitous since the analysis leading in Ref. 27 to the value quoted took no account of the quadrupole interactions which have played a fundamental role in our analysis.

## ACKNOWLEDGMENT

It is a pleasure to acknowledge the technical assistance throughout this project of John Watson.

<sup>27</sup> J. H. Pifer, Phys. Rev. **166**, 540 (1968).

## Specific Heat of Antimony and Bismuth between 0.03 and 0.8 K<sup>†</sup>

H. K. COLLAN, M. KRUSIUS, AND G. R. PICKETT

*Department of Technical Physics, Technical University of Helsinki, Otaniemi, Finland*

(Received 24 November 1969)

The specific heats of the semimetals antimony and bismuth have been measured from 0.03 to 0.8 K. The best fit to the antimony data yields  $C_p = 4.55T^{-2} + 119T + 180T^3 \mu\text{J}/\text{mole K}$ . The  $T^{-2}$  term associated with the nuclear quadrupole interaction is in good agreement with NMR measurements and also with theoretical predictions of the electric field gradient at the nucleus. The best fit for bismuth gives  $C_p = 0.0064T^{-2} + 8.5T + 1120T^3 \mu\text{J}/\text{mole K}$ . The value of the coefficient of the electronic specific heat is in agreement with predictions from Fermi-surface parameters. Slow spin-lattice relaxation in bismuth prevents the nuclear quadrupole Schottky anomaly from being observed in a calorimetric measurement.

## I. INTRODUCTION

THE semimetals antimony and bismuth crystallize in similar rhombohedral structures,<sup>1</sup> the "arsenic structure," and exhibit many similar properties. By virtue of a small band overlap, which spills a small number of electrons into the conduction band, both metals show weak metallic properties. The Fermi surfaces consist of small pockets of electrons and holes with low densities of states at the Fermi level resulting in electronic specific heats considerably lower than those of normal metals. Both metals also have isotopes with sizable nuclear quadrupole moments which interact

with the electrical field gradient (efg) at the site of the nucleus giving rise to hyperfine splittings of the order of a few tenths of a milli-Kelvin.

The quadrupole coupling constants  $e^2qQ$  have been measured by resonance techniques for both metals.<sup>2,3</sup> No precise calorimetric confirmation of the resonance figures has been made for antimony except for estimates<sup>4,5</sup> from measurements in the He<sup>3</sup> range which are, of necessity, rather inaccurate owing to the smallness of the nuclear specific heat at these temperatures. Calorimetric measurements on bismuth<sup>6</sup> have been extended

<sup>2</sup> R. R. Hewitt and B. F. Williams, Phys. Rev. **129**, 1188 (1963).

<sup>3</sup> B. F. Williams and R. R. Hewitt, Phys. Rev. **146**, 286 (1966).

<sup>4</sup> D. C. McCollum and W. A. Taylor, Phys. Rev. **156**, 782 (1967).

<sup>5</sup> R. S. Blewer, N. H. Zebouni, and C. C. Grenier, Phys. Rev. **174**, 700 (1968).

<sup>6</sup> N. E. Phillips, Phys. Rev. **118**, 644 (1960).

<sup>†</sup> Research sponsored, in part, by U. S. government under Grant No. EOOAR-69-0054. A preliminary report of the work on bismuth has appeared in Phys. Rev. Letters (Ref. 8).

<sup>1</sup> W. B. Pearson, *Lattice Spacings and Structures of Metals* (Pergamon Press, Inc., New York, 1958).

to lower temperatures but yield a coupling constant a factor of 2 lower than the resonance data would suggest. With this in view, we have measured the specific heats of antimony and bismuth in the temperature range 0.03–0.8 K.

The arsenic structure has axial symmetry about each ionic site and, thus, the quadrupole interaction can be represented by the Hamiltonian

$$H = [3e^2qQ/4I(2I-1)][I_z^2 - \frac{1}{3}I(I+1)]. \quad (1)$$

The interaction lifts the degeneracy of the  $2I+1$  nuclear spin levels giving rise to a Schottky anomaly in the heat capacity, the two leading high-temperature terms of which are<sup>6</sup>

$$\frac{C}{R} = \frac{1}{80} \frac{(2I+2)(2I+3)}{2I(2I-1)} \left( \frac{e^2qQ}{kT} \right)^2 - \frac{1}{1120} \frac{(2I-3)(2I+2)(2I+3)(2I+5)}{(2I)^2(2I-1)^2} \left( \frac{e^2qQ}{kT} \right)^3. \quad (2)$$

The magnitude of the coupling constant can be obtained from the  $T^{-2}$  term but, for the sign to be determined, the  $T^{-3}$  term must also be resolved.

Provided that the nuclear quadrupole moment is known, the coupling constant immediately gives the efg at the nucleus and, thus, provides information on the electrical structure of the material.

There are three principal contributions to the efg: (a) the contribution arising from the surrounding lattice of charged ionic cores; (b) the contribution from the conduction electrons; and (c) the modification of (a) and (b) arising from the polarizability of the host ion core.

The contribution of the charged lattice can be directly calculated as a sum over all ions. The conduction-electron term, however, requires a knowledge of the electronic wave functions, as the total charge density comes into the problem and not just that due to electrons near the Fermi surface. The polarizability or antishielding factors<sup>7</sup> have been calculated for several atoms but, where no calculations exist, an estimate can be made. Of the external contribution, the part due to the conduction electrons is usually much larger than that due to the ion cores. Thus, the experimental value of the efg can be a valuable check on any assumptions about the conduction-electron wave functions in the metal.

During the course of the measurement, it was discovered that, in the case of bismuth, the low conduction-electron density gives rise to such slow spin-lattice relaxation that the nuclear quadrupole heat capacity cannot be observed by calorimetric methods, as the nuclear system is effectively isolated.<sup>8</sup> However, this

allowed a more precise determination of the electronic heat capacity  $\gamma T$ . The coefficient  $\gamma$  is directly related to the density of states at the Fermi level through the expression

$$\gamma = \frac{1}{3}\pi^2 k^2 N(E_F), \quad (3)$$

where  $k$  is Boltzmann's constant and  $N(E_F)$  is the density of states at the Fermi energy  $E_F$ . Previous values of  $\gamma$ <sup>6,9</sup> have been in considerable disagreement with the accepted picture of the Fermi surface.

The electron surface of bismuth can be satisfactorily described by three equivalent ellipsoids with one minor axis of each ellipsoid lying along a reciprocal-lattice binary axis and the other two being tilted approximately  $6^\circ$  from the bisectrix and trigonal axes.<sup>10</sup> Assuming that the band is parabolic, which is not strictly true in this case, then the constant energy surface corresponding to one electron ellipsoid can be written

$$2m_0E_e = \alpha_{11}p_x^2 + \alpha_{22}p_y^2 + \alpha_{33}p_z^2 + 2\alpha_{23}p_y p_z, \quad (4)$$

where  $\alpha$  is the inverse mass tensor  $1/m^*$ . Similar expressions can be obtained for the other two electron surfaces by a  $\pm 120^\circ$  rotation about the trigonal axis.

The hole surface is also an ellipsoid with its major axis parallel to the trigonal axis. The constant energy surface can be written

$$2m_0E_h = \beta_1(p_x^2 + p_y^2) + \beta_3p_z^2, \quad (5)$$

where  $\beta$  is the inverse mass tensor for the holes.

The density of states can be directly calculated from Eqs. (4) and (5) to give

$$N(E_F) = \left( \frac{24\pi V}{h^3} \right) \frac{(2E_{eF})^{1/2} m_0^{3/2}}{(\alpha_1\alpha_2\alpha_3)^{1/2}} + \left( \frac{8\pi V}{h^3} \right) \frac{(2E_{hF})^{1/2} m_0^{3/2}}{(\beta_1\beta_3)^{1/2}}, \quad (6)$$

where  $\alpha_1$ ,  $\alpha_2$ , and  $\alpha_3$  are now the values of  $\alpha$  corresponding to the principal axes of the ellipsoid, and the difference in the numerical factor between the electron and hole expressions is due to the fact that there are three electron surfaces and only one for the holes.

Retaining the assumption of parabolic bands, the density of states can also be written as a simple function of the total number of states enclosed by the surfaces

$$N(E_F) = \frac{3}{2}(n_e/E_{eF} + n_h/E_{hF}), \quad (7)$$

where  $n_e$  and  $n_h$  are, respectively, the total numbers of conduction electrons and holes below the Fermi level. This expression gives  $N(E_F)$  in terms of quantities not dependent on the precise ellipsoid geometry. For charge neutrality, we can assume that  $n_e$  and  $n_h$  are equal provided that the material is pure. The total carrier

<sup>7</sup> R. M. Sternheimer, Phys. Rev. **80**, 102 (1950); **84**, 244 (1951); **86**, 316 (1952).

<sup>8</sup> H. K. Collan, M. Krusius, and G. R. Pickett, Phys. Rev. Letters **23**, 11 (1969).

<sup>9</sup> I. N. Kalinkina and P. G. Strelkov, Zh. Eksperim. i Teor. Fiz. **34**, 616 (1958) [English transl.: Soviet Phys.—JETP **7**, 426 (1958)].

<sup>10</sup> D. Schoenberg, Proc. Roy. Soc. (London) **A170**, 341 (1939).

density can be obtained from infrared absorption and Alfvén wave measurements. Values for the two Fermi energies are well known from a variety of experiments.

The expected electronic heat capacity can thus be calculated using either the experimental value of  $n_e$  and Eq. (7) or the experimental values of the inverse mass tensor elements and Eq. (6). Values of  $\gamma$  so calculated show reasonable agreement with each other but are much lower than existing experimental values. This disagreement has been rather puzzling and to explain the discrepancy extra bands of carriers have been proposed and searched for experimentally,<sup>11</sup> although no such bands have been unambiguously identified.

## II. EXPERIMENTAL DETAILS

The measurements were made in an adiabatic demagnetization cryostat with a He<sup>3</sup> precooling stage. The inner parts are shown in Fig. 1. Somewhat different arrangements were used for the two metals.

For the antimony runs, the specimen was thermally anchored to the cooling salt via a superconducting switch of 0.5-mm-diam high-purity tin wire actuated by a small superconducting solenoid. Two switches of different lengths were used for the high- and low-temperature regions to keep the drift rate of the specimen within reasonable bounds over the whole temperature range. Contact to the specimen itself was made by a copper foil wrapped around the upper end of the specimen and tightly bound with terylene thread, the contacting surfaces being wetted with an amalgam of Hg-In-Tl.

The sample temperature was measured by a cerium magnesium nitrate (CMN) thermometer consisting of a bundle of single crystals interleaved with coil foils<sup>12</sup> liberally coated with Apiezon *N* grease, also attached to the specimen by a cold-soldered copper foil. The specimen heater was a 90%Pt-10%W wire wound non-inductively around the specimen and anchored with *N* grease. The current leads to the heater were superconducting. The salt pill and the rigidly held coil-foil heat shield were supported on threads from a cradle at the temperature of the He<sup>3</sup> pot. The specimen was also supported rigidly on threads from the heat shield liner.

The CMN thermometer was calibrated against the vapor pressure of He<sup>3</sup> between 0.8 and 1.9 K, while the He<sup>3</sup> pot temperature was stabilized by an electronic regulator. The calibration was accurate to 0.2% with an additional error of  $\pm 0.5$  mK arising from the uncertainty in the shape factor of the thermometer. After calibration, the He<sup>3</sup> exchange gas was pumped out and the cooling salt magnetized. Demagnetization proceeded in stages, taking some 5 h for the lower temperature runs. When the specimen was cool, the heat switch was

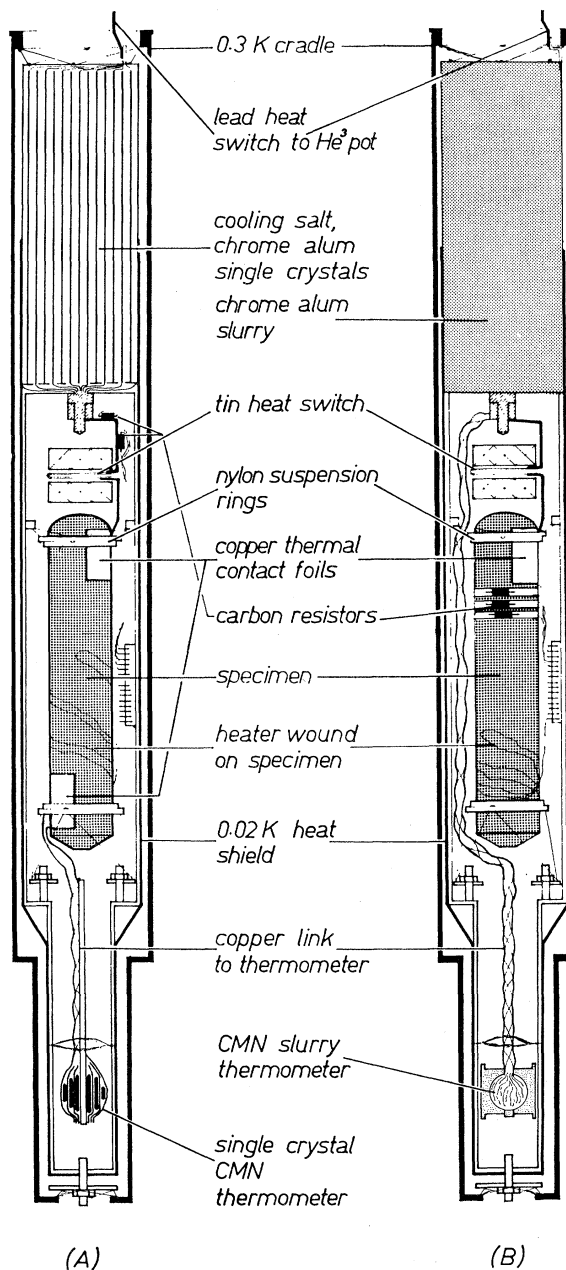


FIG. 1. Experimental arrangement (A) for antimony, and (B) for bismuth.

opened and heat pulse measurements were made in the usual way.

The addenda consisted principally of the copper foils and coil foils, the CMN thermometer crystals, and the nylon suspension rings around the specimen, the heat capacity of which was measured in a separate experiment. An accurate knowledge of the addenda heat capacity is necessary as it contributes about 7% of the total heat capacity at the lower temperatures, rising to about 40% at 0.7 K.

<sup>11</sup> L. S. Lerner, Phys. Rev. **127**, 1480 (1962); **130**, 605 (1963).

<sup>12</sup> Coil foil is a sheet of fine insulated copper wires laid parallel and bonded with varnish, giving good thermal conductance along the wires with a low susceptibility to eddy current heating.

The main features of the bismuth experiment were similar to those for antimony with a few notable exceptions. The use of a CMN thermometer directly attached to the sample would have resulted in a prohibitively high addenda correction from the  $T^{-2}$  term in the CMN heat capacity, and instead the temperature was monitored by carbon resistors. Three Speer resistors were used, two 220  $\Omega$  0.5 W and one 51  $\Omega$  0.5 W, anchored by Apiezon *N* grease in holes drilled in the specimen. The outer plastic casing was ground off and the carbon pellets insulated with a thin layer of Araldite. One of the 220- $\Omega$  resistors had all but 10% of the length of the carbon pellet shorted by conducting paint to give a reasonable resistance at the lower temperatures while retaining the high sensitivity of the original resistor. This latter was found to have the most convenient characteristics and was used exclusively in the measurement.

The resistors were calibrated against a CMN thermometer in thermal contact with the cooling salt, the large heat capacity of which was used as thermal ballast for achieving equilibrium during calibration. While calibrating, the heat switch was maintained in the conducting state and various powers were fed to the specimen heater to make certain that the stray heat leak did not establish a significant temperature difference ( $>0.3$  mK) between the CMN thermometer and the carbon resistors. The CMN thermometer consisted of a slurry of CMN powder, saturated aqueous solution, and glycerol, contained in a spherical Epibond cavity. Thermal contact to the cooling salt was made by a bundle of 0.07-mm-diam copper wires. This particular form of thermometer was chosen to speed up the slow response of the single-crystal arrangement and also to reduce the shape correction.

### III. RESULTS AND DISCUSSION

#### A. Antimony

The antimony specimen, weighing 291 g (2.4 moles), was cast in a high-purity graphite mold into a cylinder 24 mm in diameter and 98 mm long and consisted of a few large crystals. The starting material was 99.9999% zone refined grade antimony from Koch Light Laboratories. After casting, the purity was checked by mass spectrometry and was found to be better than 99.999%. The resistance ratio  $\rho_{300}/\rho_{4.2}$  was greater than 2000.

The results are plotted in Fig. 2 and listed in Table I. Measurements were taken down to about 19 mK, but the thermal equilibrium times of the specimen and thermometer together became so long, due presumably to slow nuclear spin-lattice relaxation, that large systematic errors appeared from the overheating of the lattice and consequent large heat loss to the surroundings. For this reason, we discarded all points taken below 38 mK where the time required for establishing thermal equilibrium after a heat pulse was about 2000

TABLE I. Measured specific heat of antimony in  $\mu\text{J}/\text{mole K}$ .

$T$ (K)	$C_p$	$T$ (K)	$C_p$	$T$ (K)	$C_p$
0.0396	2954	0.1011	461.0	0.3568	85.25
0.0411	2730	0.1027	446.2	0.3597	85.43
0.0421	2604	0.1028	444.3	0.3605	84.38
0.0428	2522	0.1034	445.6	0.3685	85.60
0.0455	2230	0.1036	434.2	0.3865	86.53
0.0471	2073	0.1120	382.9	0.3911	84.86
0.0480	2026	0.1121	379.4	0.3912	86.16
0.0482	1986	0.1133	375.0	0.3997	85.36
0.0500	1836	0.1134	373.0	0.4029	86.97
0.0507	1787	0.1158	361.1	0.4125	88.27
0.0511	1768	0.1208	331.0	0.4336	91.47
0.0546	1535	0.1229	315.0	0.4342	91.30
0.0560	1452	0.1229	316.1	0.4436	91.61
0.0566	1443	0.1316	282.5	0.4452	89.98
0.0568	1425	0.1353	265.8	0.4616	92.78
0.0575	1400	0.1441	235.1	0.4713	95.64
0.0595	1297	0.1550	206.3	0.4772	97.10
0.0596	1320	0.1637	190.1	0.4815	98.74
0.0603	1272	0.1763	168.4	0.4911	99.34
0.0611	1233	0.1789	166.9	0.5055	101.2
0.0638	1146	0.1915	149.2	0.5179	103.0
0.0653	1070	0.1938	148.1	0.5292	104.2
0.0659	1054	0.2060	135.2	0.5327	106.9
0.0666	1042	0.2246	119.2	0.5376	108.4
0.0668	1018	0.2333	115.0	0.5556	112.0
0.0687	978.1	0.2397	111.5	0.5614	114.7
0.0727	871.9	0.2413	109.7	0.5821	120.6
0.0729	858.9	0.2420	110.9	0.5843	119.9
0.0734	853.1	0.2529	105.6	0.6139	125.9
0.0768	787.8	0.2536	104.3	0.6269	136.5
0.0771	784.5	0.2704	99.18	0.6297	134.7
0.0785	746.0	0.2920	93.50	0.6676	144.0
0.0790	739.5	0.2979	91.40	0.6788	144.6
0.0844	648.3	0.2980	90.37	0.7015	159.6
0.0878	600.6	0.3059	90.83	0.7370	173.3
0.0899	568.5	0.3060	91.66	0.7395	175.5
0.0907	560.9	0.3098	91.07	0.7698	176.9
0.0939	525.3	0.3471	86.53	0.7758	187.3
0.0992	472.8	0.3487	86.92	0.7848	181.7
0.1001	463.4	0.3523	86.05		

sec. The measured heat input  $Q$  was fitted to an expression of the form

$$Q = \int_{T_i}^{T_f} C_p dT, \quad (8)$$

where  $T_i$  and  $T_f$  are the initial and final temperatures extrapolated to the middle of the heating period. The total specific heat was represented by

$$C_p = AT^{-2} + \gamma T + \alpha T^3, \quad (9)$$

where the three terms correspond to the nuclear, electronic, and phonon contributions, respectively. The best fit gave (in  $\mu\text{J}/\text{mole K}$ )

$$C_p = (4.55 \pm 0.09)T^{-2} + (119 \pm 7)T + (180 \pm 31)T^3.$$

The uncertainty limits of the parameters are statistical standard deviations. These errors are mainly determined by the precision with which the addenda could be measured. The separate measurement of the addenda gave  $C_{\text{add}}(\mu\text{J}/\text{mole K}) = (0.792 \pm 0.09)T^{-2} + (200 \pm 7)T + (136 \pm 35)T^3$ .

The shape correction of the thermometer,  $\Delta$ , was also determined in the fitting process by setting  $T = T^* + \Delta$ ,

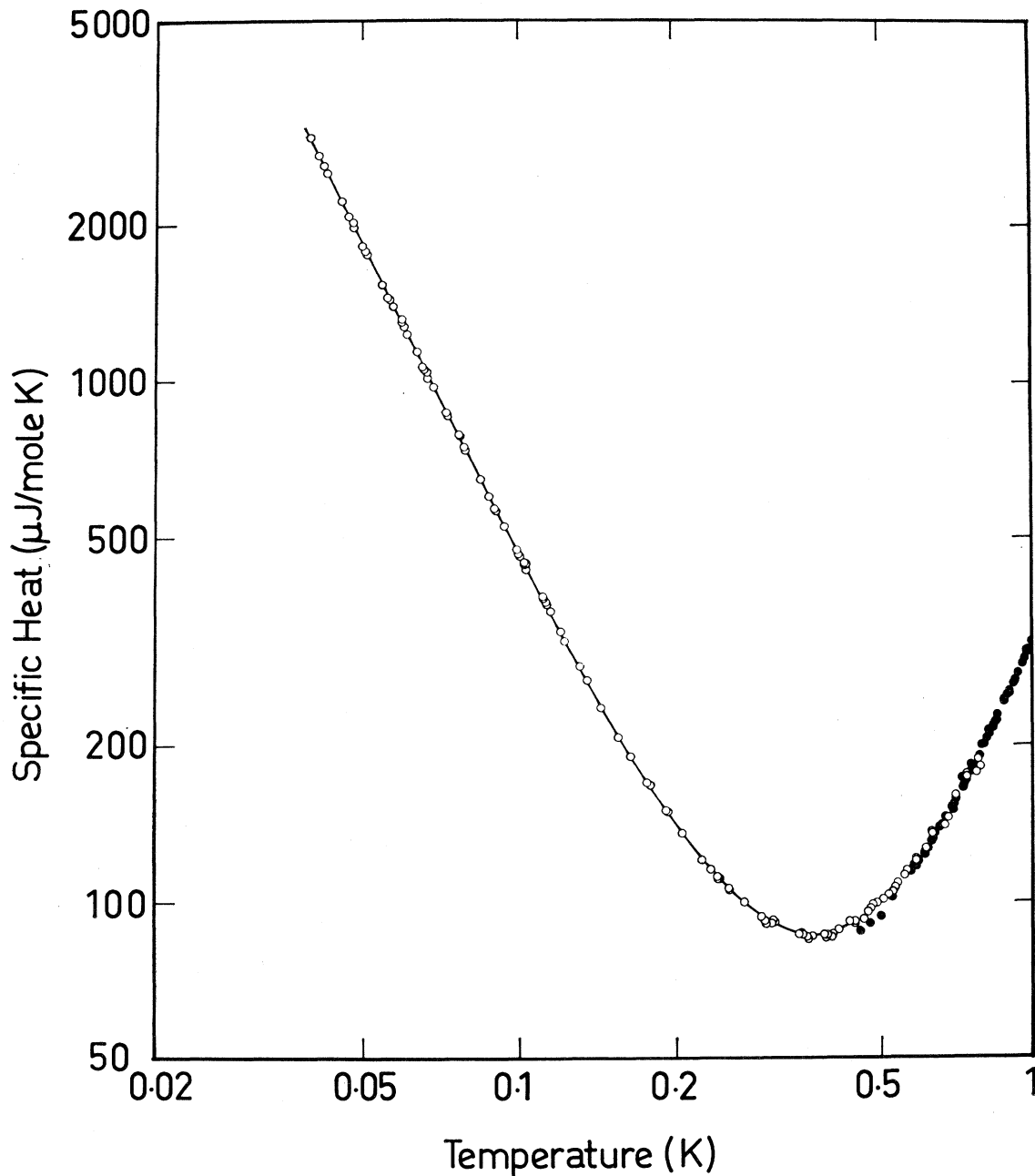


FIG. 2. Measured specific heat of antimony versus temperature. The symbol  $\circ$  represents data from this work and the measurements of both McCollum and Taylor (Ref. 4) and Culbert (Ref. 17), being almost congruent, are indicated by the symbol  $\bullet$ . The full curve represents the best fit to our data as discussed in the text.

where  $T^*$  is the magnetic temperature as indicated by the CMN thermometer. The value thus obtained for  $\Delta$  of  $2.3 \pm 0.5$  mK is comparable to that reported by Anderson for a similar thermometer also consisting of a bundle of single crystals.<sup>13</sup> The values of the parameters  $A$ ,  $\gamma$ , and  $\alpha$  in (8) for antimony are listed in Table II

<sup>13</sup> A. C. Anderson, J. Appl. Phys. **39**, 5878 (1968).

along with those of other recent measurements at higher temperatures.

The  $T^{-2}$  term is in agreement with the He<sup>3</sup> range measurement of McCollum and Taylor<sup>4</sup> but considerably higher than the figure given by Blewer *et al.*<sup>5</sup> Assuming isotopic abundances of 57.25% Sb<sup>121</sup> and 42.75% Sb<sup>123</sup>, and taking for the ratio of the quadrupole moments  $Q^{121}/Q^{123}$  the value of 0.7844 from the NMR

measurements of Hewitt and Williams,<sup>2</sup> we obtain from the present results coupling constants  $e^2qQ^{121}$  and  $e^2qQ^{123}$  of  $3.77 \pm 0.04$  and  $4.80 \pm 0.05$  mK, compared with the resonance values of 3.68836 and 4.70236 mK.<sup>2</sup> The two measurements are in good agreement, although the 2% discrepancy is well outside the error limits of either experiment. It is difficult to believe that the differences in the form of the metal used in the two measurements, 325-mesh powder in the resonance and a massive cylinder in the calorimetric case, could lead to a variation in the efg of this order.

The extraction of the field gradient from the coupling constant requires a knowledge of the quadrupole moments  $Q$  which, unfortunately, are not very precisely known. However, taking the values  $Q^{121} = -0.52 \times 10^{-24}$  cm<sup>2</sup> and  $Q^{123} = -0.67 \times 10^{-24}$  cm<sup>2</sup> from the measurement of Murakawa,<sup>14</sup> we get a figure of  $2080 \times 10^{12}$  esu (averaged over both isotopes) for the efg at the nucleus. The ionic contribution to the efg has been calculated by Taylor and Hygh,<sup>15</sup> and the electronic contribution calculated and the antishielding factors estimated by Hygh and Das<sup>16</sup> giving a total calculated efg of  $1900 \times 10^{12}$  esu which is in good agreement with the calorimetric and resonance values, although this is probably fortuitous owing to the uncertainties in the quadrupole moments. It is unfortunate that the long equilibrium times prevented the present measurements from being made much below 40 mK, as at this temperature the  $T^{-3}$  term of Eq. (2) is only some 0.8% of the  $T^{-2}$  term and, thus, is too small to be satisfactorily resolved. Consequently, the sign of the interaction could not be determined.

The temperature range over which the nuclear heat capacity does not dominate is rather short in the present measurements, and the electronic and phonon contributions to the specific heat cannot be very precisely separated from each other, as indicated by the relatively large error limits assigned. However, as can be seen in Fig. 2, the measured points agree well at the higher temperatures with those of McCollum and Taylor<sup>4</sup> and Culbert<sup>17</sup> which is not so obvious from the fitted parameters of Table II.

TABLE II. Recent experimental values of the coefficients  $A$ ,  $\gamma$ , and  $\alpha$  in the expression  $C_p = AT^{-2} + \gamma T + \alpha T^3$  for antimony ( $\mu\text{J}/\text{mole K}$ ).

	McCollum <i>et al.</i> <sup>a</sup>	Culbert <sup>b</sup>	Blewer <i>et al.</i> <sup>c</sup>	This work
$A$	$4.8 \pm 0.4$	...	$1.97 \pm 0.23$	$4.55 \pm 0.09$
$\gamma$	$105 \pm 2$	$112 \pm 5$	$116.5 \pm 6.4$	$119 \pm 7$
$\alpha$	$210 \pm 2$	$206 \pm 1$	$211 \pm 5.3$	$180 \pm 31$

<sup>a</sup> Reference 4.  
<sup>b</sup> Reference 17.  
<sup>c</sup> Reference 5.

<sup>14</sup> K. Murakawa, Phys. Rev. **93**, 1232 (1954).

<sup>15</sup> T. T. Taylor and E. H. Hygh, Phys. Rev. **129**, 1193 (1963).

<sup>16</sup> E. H. Hygh and T. P. Das, Phys. Rev. **143**, 452 (1966).

<sup>17</sup> H. V. Culbert, Phys. Rev. **157**, 560 (1967).

TABLE III. Measured specific heat of bismuth in  $\mu\text{J}/\text{mole K}$ . The dynamically measured points are not listed.

$T$ (K)	$C_p$	$T$ (K)	$C_p$	$T$ (K)	$C_p$
0.0739	2.342	0.1231	3.434	0.2500	20.74
0.0774	1.883	0.1271	3.423	0.2608	22.06
0.0784	1.981	0.1272	3.497	0.2631	23.02
0.0897	2.214	0.1407	5.095	0.2722	26.18
0.0905	2.412	0.1447	4.896	0.2733	25.84
0.0907	2.344	0.1460	4.647	0.2961	31.37
0.0908	2.258	0.1616	6.520	0.3021	34.32
0.0932	2.381	0.1652	5.947	0.3158	37.88
0.0955	2.474	0.1660	7.238	0.3223	39.84
0.0967	2.332	0.1742	7.040	0.3480	49.20
0.1007	2.651	0.1803	7.779	0.3593	55.11
0.1010	2.230	0.1875	9.038	0.3653	57.66
0.1056	2.917	0.1894	7.669	0.4072	80.12
0.1080	2.941	0.1942	10.44	0.4108	80.30
0.1096	2.670	0.1964	10.04	0.4788	127.1
0.1097	2.596	0.1965	10.23	0.4903	134.3
0.1116	3.156	0.2073	12.47	0.5326	171.0
0.1215	3.796	0.2191	14.86	0.5406	179.3
0.1216	3.815	0.2236	14.58	0.6476	308.5
0.1222	3.530	0.2290	16.05	0.7229	428.6
0.1224	3.491	0.2307	16.99	0.7705	517.0
0.1231	3.443				

## B. Bismuth

The bismuth specimen, weighing 495 g (2.4 moles), was prepared in the same way as the antimony specimen. The starting material was 99.9999% zone refined grade bismuth from Koch Light Laboratories. The final purity after casting was better than 99.999%. The specimen consisted of a few large crystals and had a resistance ratio of 230.

The results are presented in Fig. 3 and Table III. Owing to the very small heat capacity at the lower temperatures, conventional heat pulse measurements could not be made and two other methods, to be described more fully elsewhere, were used. We include only a brief description of the two methods here. As the specific heat can be represented by an expression of the form  $C_p = AT^{-2} + \gamma T + \alpha T^3$ , heat pulse measurements need not be restricted to small temperature intervals. To take advantage of this, the specimen was heated to a final temperature  $T_f$  which was several times the initial temperature  $T_i$ , and  $C_p$  was then fitted to the total heat input to the specimen  $Q(T_f, T_i)$  in the integral form

$$Q(T_f, T_i) = \int_{T_i}^{T_f} C_p(T) dT. \quad (10)$$

The correction for the heat leak to the specimen during the heating periods was not made by an extrapolation procedure, which was impossible owing to the curvature of the drifts, but by fitting a polynomial in  $T$  to the drift curves before and after the heating period to determine the heat-leak rate as a function of temperature. The best fit gave (in  $\mu\text{J}/\text{mole K}$ )  $C_p = (0.0064 \pm 0.0010)T^{-2} + (8.5 \pm 1.5)T + (1120 \pm 25)T^3$ , where the uncertainty limits of the parameters are standard deviations. The filled points in Fig. 3 represent these integral

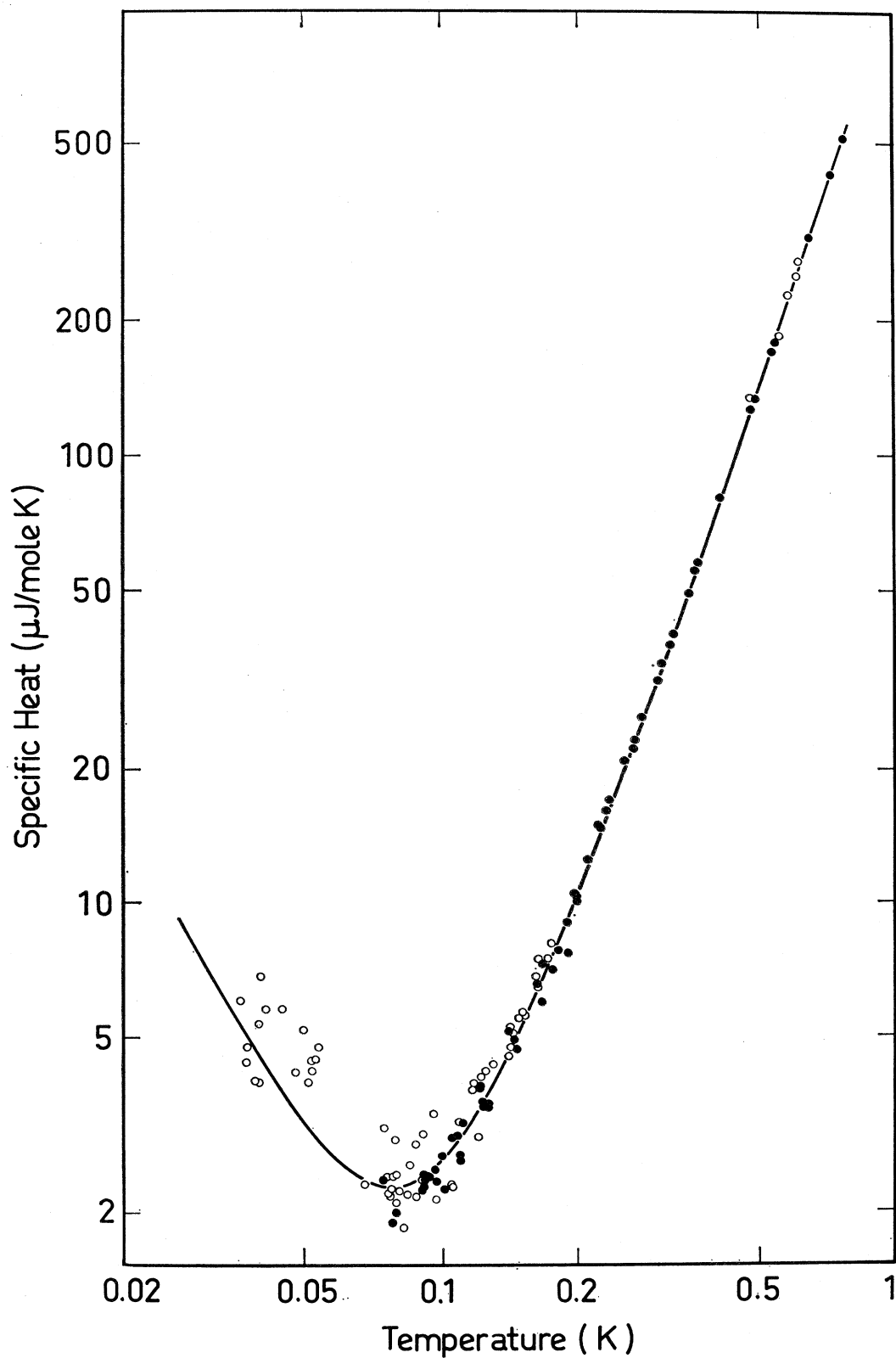


FIG. 3. Measured specific heat of bismuth versus temperature. The symbol ● represents integral determinations and ○ indicates dynamic determinations (for the significance of the measuring method, see text). The curve represents the best fit to the integral data.

measurements. The integral in each case has been reduced to a point value at the midpoint  $\bar{T}$  of the heating interval by the relation

$$C_p(\bar{T}) = \frac{C(\bar{T})_{\text{calc}} Q(T_f, T_i)_{\text{meas}}}{Q(T_f, T_i)_{\text{calc}}}, \quad (11)$$

where  $Q(T_f, T_i)_{\text{meas}}$  is the measured heat input to the specimen, corrected for the heat leak to the surroundings, and  $Q(T_f, T_i)_{\text{calc}}$  and  $C(\bar{T})_{\text{calc}}$  are calculated from the best-fit parameters.

As a check on the above measurements, a dynamic method was also used. In this case, the specimen was approximately stabilized at the desired temperature by carefully adjusting the heat switch solenoid current to leave the switch in a partially conducting state. The drift rate of the specimen was then recorded before and after a sudden change in the power  $P$ , delivered to the specimen heater. In this case, the change in drift rate gives the heat capacity through the relation

$$C_p(dT_1/dt - dT_2/dt) = (P_1 - P_2). \quad (12)$$

These measurements are represented by the open circles in Fig. 3. They were not included in the fitting of the parameters.

The addenda in the case of bismuth consisted only of the 0.868 g of copper in the thermal contact foils, the thermal contact amalgam, the nylon support rings, terylene thread, and the carbon resistors. It was impossible to measure these rather small quantities and, in this case, the correction to the heat capacity was calculated from the known heat capacities of the various components.

The best-fit parameters are listed in Table IV along with those of other recent measurements. The  $T^{-2}$  term expected from the NMR measurements of Williams and Hewitt<sup>3</sup> is not observed and this we attribute to slow spin-lattice relaxation due to the low electron density in bismuth. By careful analysis of the drift curves, we attempted to estimate the relaxation time  $\tau_1$ . This, however, is very long, and we can only set a lower limit of  $100/T$  sec. The small  $T^{-2}$  term of the present measurements and also that of Phillips is undoubtedly associated with nuclear contributions to the heat capacity from the addenda.

The phonon contribution is in excellent agreement with Phillips's value and also within the uncertainty limits with that of Kalinkina and Strelkov.<sup>9</sup> The electronic term, however, is considerably lower than values reported earlier and is much more in line with estimates from Fermi-surface parameters. Using Eq. (3) and

TABLE IV. Recent experimental values for the coefficients  $A$ ,  $\gamma$ , and  $\alpha$  in the expression  $Cp = AT^{-2} + \gamma T + \alpha T^3$  for bismuth ( $\mu\text{J}/\text{mole K}$ ).

	Kalinkina <i>et al.</i> <sup>a</sup>	Phillips <sup>b</sup>	This work
$A$	...	0.28	$0.0064 \pm 0.0010$
$\gamma$	$67.0 \pm 0.5$	21	$8.5 \pm 1.5$
$\alpha$	$1170 \pm 40$	1114	$1120 \pm 25$

<sup>a</sup> Reference 9.  
<sup>b</sup> Reference 6.

substituting (7) for the density of states, we have an expression for  $\gamma$ , directly from the Fermi energies  $E_{eF}$  and  $E_{hF}$  and the total densities of the two types of carriers which we assume to be equal. Taking representative values for  $E_{eF}$  and  $E_{hF}$  of 27.6 and 10.9 meV from Smith *et al.*<sup>18</sup> and  $n_e = n_h = 3.10 \times 10^{17} \text{ cm}^{-3}$  from the Alfvén wave measurements of Williams,<sup>19</sup> we obtain a value of  $5.0 \mu\text{J}/\text{mole K}^2$  for  $\gamma$ . If we instead use for the density of states the expression of Eq. (6), which is more specifically in terms of the Fermi-surface geometry, and take the values (in units of  $m_0^{-1}$ ) 141, 0.584, 87.3, 14.8, and 1.32 for  $\alpha_1, \alpha_2, \alpha_3, \beta_1$ , and  $\beta_3$ , respectively, given by Kao,<sup>20</sup> we find  $\gamma = 6.8 \mu\text{J}/\text{mole K}^2$ . In view of the uncertainties in the various quantities used in these two calculations and the assumption of the parabolic-band ellipsoid model, the agreement is quite good.

Our measured figure for  $\gamma$  of  $8.5 \pm 1.5 \mu\text{J}/\text{mole K}^2$ , even allowing for the large uncertainty, falls somewhat above the calculated values. The assumption made when calculating the addenda correction that the heat capacity of the 0.87 g of copper in the calorimeter can be taken as that of the pure material probably underestimates this contribution which would make the true value of  $\gamma$  somewhat lower. However, the agreement with the calculated values is very much better than that of the earlier measurements, as can be seen from Table IV, and the conventional picture of the Fermi surface is substantially confirmed, ruling out the possibility of bands of "heavy" holes as suggested by Lerner.<sup>11</sup>

#### ACKNOWLEDGMENTS

The authors are grateful to T. Heikkilä for assisting in the calculation of the results, to P. Gregers-Hansen for several useful discussions, and would like to acknowledge the encouraging interest of Professor O. V. Lounasmaa at all stages of this work.

<sup>18</sup> G. E. Smith, G. A. Baraff, and J. M. Rowell, Phys. Rev. **135**, A1118 (1964).

<sup>19</sup> G. A. Williams, Phys. Rev. **139**, A771 (1965).

<sup>20</sup> Y.-H. Kao, Phys. Rev. **129**, 1122 (1963).